

Optimal reconstruction interval in dual source CT coronary angiography: a single-center experience in 285 patients

Ayça Akgöz, Deniz Akata, Tuncay Hazırolan, Muşturay Karçaaltıncaba

PURPOSE

We aimed to evaluate the visibility of coronary arteries and bypass-grafts in patients who underwent dual source computed tomography (DSCT) angiography without heart rate (HR) control and to determine optimal intervals for image reconstruction.

MATERIALS AND METHODS

A total of 285 consecutive cases who underwent coronary (n=255) and bypass-graft (n=30) DSCT angiography at our institution were identified retrospectively. Patients with atrial fibrillation were excluded. Ten datasets in 10% increments were reconstructed in all patients. On each dataset, the visibility of coronary arteries was evaluated using the 15-segment American Heart Association classification by two radiologists in consensus.

RESULTS

Mean HR was 76 ± 16.3 bpm, (range, 46–127 bpm). All coronary segments could be visualized in 277 patients (97.19%). On a segment-basis, 4265 of 4275 (99.77%) coronary artery segments were visible. All segments of 56 bypass-grafts in 30 patients were visible (100%). Total mean segment visibility scores of all coronary arteries were highest at 70%, 40%, and 30% intervals for all HRs. The optimal reconstruction intervals to visualize the segments of all three coronary arteries in descending order were 70%, 60%, 80%, and 30% intervals in patients with a mean HR <70 bpm; 40%, 70%, and 30% intervals in patients with a mean HR 70–100 bpm; and 40%, 50%, and 30% in patients with a mean HR >100 bpm.

CONCLUSION

Without beta-blocker administration, DSCT coronary angiography offers excellent visibility of vascular segments using both end-systolic and mid-late diastolic reconstructions at HRs up to 100 bpm, and only end-systolic reconstructions at HRs over 100 bpm.

Improvements in computed tomography (CT) scanning technology throughout the last decade have resulted in widespread acceptance of contrast-enhanced multidetector CT (MDCT) coronary angiography as a reliable modality for noninvasive evaluation of the coronary arteries (1). Having a high negative predictive value, MDCT coronary angiography is considered particularly beneficial in patients with low to intermediate pretest probability for coronary artery disease (CAD) by reliably excluding coronary artery stenosis and therefore, preventing unnecessary invasive angiography (2, 3).

Small dimensions and continuous rapid motions of coronary arteries make their visualization by CT challenging. Thus, excellent spatial and temporal resolution is required for adequate imaging of coronary arteries. Initial reports using a 4-detector row MDCT were promising in selected patients with low heart rates (HRs) (4–6); however, image quality was not sufficient for assessment in up to 29% of the coronary segments. With the introduction of 16- and 64-row MDCT, major improvements of image quality were achieved, with adequate visualization of up to 97% of coronary segments (7–9). Since, image quality deteriorates with increasing HRs even with 64-slice MDCT scanners (10, 11), it has been common in clinical practice to use HR-modulating beta-blockers to achieve better diagnostic quality. In 2005, dual source CT (DSCT) system equipped with two sets of X-ray tubes and corresponding detectors mounted onto the gantry with an angular offset of 90° was introduced (12). Using half-scan reconstruction algorithms, this system provides high temporal resolution (83 milliseconds [ms]) that corresponds to a quarter gantry rotation time. Preliminary studies without use of beta-blocker premedication have shown that DSCT coronary angiography provides good image quality of coronary arteries even at a relatively high HR (13, 14). Subsequent studies with relatively small patient populations confirmed these findings with diagnostic image quality in 97.8% of coronary artery segments (15, 16).

Achievement of good image quality with DSCT coronary angiography is highly dependent upon selecting the optimal reconstruction interval for evaluation. Previous publications indicate a relationship between optimal reconstruction window and HR with mid- to end-diastolic reconstructions providing better image quality at low HRs, whereas at faster HRs, end-systolic reconstructions will often provide the dataset with the least motion artifact (17–19). However, some of these prior studies were based on relatively small patient samples, and in some, the entire R-R interval was not evaluated. Detection of optimal reconstruction interval is also important for the purpose of radiation dose reduction. Since DSCT scanners are equipped with electrocardiogram (ECG)-based tube

Department of Radiology (M.K. ✉ musturayk@yahoo.com), Hacettepe University School of Medicine, Ankara, Turkey.

Received 12 November 2013; revision requested 24 November 2013; revision received 15 January 2014; accepted 22 January 2014.

Published online 8 May 2014.
DOI 10.5152/dir.2014.13451

current modulation, the width and timing of the ECG pulsing window, during which the full tube current is given, can be manually selected by the operator with the tube current outside the pulsing window decreased to 20% or 4% of the nominal tube current and thus, significantly reducing the radiation dose up to 40% (20).

We aimed to evaluate the visibility of coronary arteries and bypass-grafts in patients who underwent DSCT angiography without HR control and to determine optimal intervals for image reconstruction.

Material and methods

Study group

Approval for this retrospective study was obtained from the institutional review board, with a waiver of informed consent. Using our database, we retrospectively identified coronary and bypass-graft CT angiography (CTA) studies that were performed in our institution between December 2006 and January 2007, using DSCT (SOMATOM Definition, Siemens Medical Solutions, Forchheim, Germany). A total of 285 consecutive patients were included in our study. Patients with atrial fibrillation were excluded. Appropriate clinical data including age, gender, and study indication were collected.

Study protocol

All cardiac CTA examinations were carried out using the following technical parameters: 330 ms gantry rotation time, 0.6 mm slice and detector thickness, 0.6 mm reconstruction index, 2×32×0.6 mm detector configuration and 120 kV tube potential. Temporal resolution was 83 ms utilizing half-scan reconstruction algorithm for image acquisition. Pitch was HR-dependent (0.2–0.43) and automatically determined by the CT scanner. ECG-controlled tube current modulation was used with full tube current from 20% to 80% R-R intervals and tube current was reduced by 80% throughout the remainder of the cardiac cycle. Prior to the scan, an antecubital 18–20-gauge intravenous (IV) access was obtained for administration of IV contrast and patients' HR and rhythm were checked following connection of the ECG leads. Approximately two minutes before the

scanning, all patients were administered sublingual nitroglycerin spray to dilate the coronary arteries in order to improve visualization of the coronary arteries. The scanning delay was determined using a bolus-triggering technique (CARE Bolus, Siemens Medical Solutions). Following acquisition of the localizer image, a single unenhanced scan was obtained through the level of the aortic root with subsequent placement of a region of interest (ROI) inside the lumen of the ascending aorta. Then, utilizing an automatic injector (Missouri™, Ulrich Medical, Ulm, Germany), 70–80 mL of nonionic contrast was administered intravenously at an injection rate of 5–6 mL/s, followed by 50 mL of saline flush. Image acquisition commenced when the threshold enhancement of 100 Hounsfield unit (HU) was achieved within the ROI. Scanning was conducted in a cranio-caudal direction from the level of the carina to the level of the diaphragm during routine coronary CTA. For coronary-bypass evaluation, scan range was extended to cover the entire thorax beginning from the level of the thoracic inlet to the diaphragm. The mean scanning duration was on average 5–10 s. No complications occurred.

The effective dose of CTA was derived using the dose-length product (DLP) and a conversion coefficient ($k=0.017 \text{ mSv}\cdot\text{mGy}^{-1}\cdot\text{cm}^{-1}$) (20). Mean DLP and effective dose of the coronary CTA studies were 969.1071 mGy.cm and 16.475 mSv in bypass-graft evaluation, and 576.0576 mGy.cm and 9.79 mSv in the remaining patients.

Image analysis

Coronary and bypass CTA data post-processing was conducted offline using dedicated software (4-D INSPACE) on vendor-specific clinical image processing workstation (LEONARDO, Siemens Medical Systems, Erlangen, Germany).

Ten CT data sets in 10% increments were reconstructed for all patients throughout the entire R-R interval. Slice thickness was 0.75 mm with a reconstruction increment of 0.5 mm. For all images, a medium-soft convolution kernel (B26f) was used. Coronary arteries were classified into 15-segments according to the scheme proposed by

the American Heart Association (21). The right coronary artery (RCA), the left main and left anterior descending artery (LAD), and the left circumflex artery (LCX) were defined to include segments 1–4, segments 5–10, and segments 11–15, respectively. If there was a ramus intermedius, it was coded as first diagonal (segment 9). The images were analyzed to assess coronary artery segment visibility on each data set by two radiologists in consensus, using both axial source images and multiplanar reconstructions. Each coronary artery was graded from 0 to 4 in terms of its segment visibility; the artery was scored as "4" when all of its segments were evaluable and when unevaluable segments were present, the artery was graded as "4 minus the number of unevaluable segments", and was graded as "0" when no segments were evaluable. Coronary artery segments were categorized as evaluable if there was sufficient luminal visualization that would allow evaluation for the presence of significant stenosis. The dominance of the coronary circulation was determined by the circulation that gave rise to the posterior descending artery, and the posterolateral left ventricular branches. Bypass-grafts were classified into three segments as proximal, mid, and distal and were graded 0–3 in terms of segment visibility.

Besides dataset evaluation for segment visibility, patient demographics, clinical referral information, pretest probability for CAD (22), mean HR, ECG tracing, patient protocol including DLP, patient height and weight were all recorded. Based on the patient's ECG tracing, patient's HR variability (HRV) was calculated as the standard deviation from the average HR.

Statistical analysis

All statistical analyses were performed utilizing commercially available software (SPSS 15.0 for Windows, Chicago, Illinois, USA). A *P* value of less than 0.05 indicated a statistically significant difference. Quantitative variables were expressed as mean±standard deviation and categorical variables were expressed as frequency or percentage.

Independent samples *t* test was performed to compare the mean HR and HRV of different patient groups. For

comparison of the coronary artery visibility scores of LAD, LCX, and RCA at 10% datasets, repeated measures analysis of variance was performed first. If statistically significant difference was found between the groups, one-way analysis of variance was performed for comparison of scores at each reconstruction interval level separately.

In a similar manner, repeated measures analysis of variance was conducted to compare coronary artery segment visibility scores between patient groups with different mean HRs: <70 beats per minute (bpm), 70–100 bpm and >100 bpm. In case of statistically significant difference between the groups, one-way analysis of variance was performed for each reconstruction interval.

Results

In total, data of 285 consecutive patients (174 male, 111 female; mean age 56.5 ± 11 years; range 25–82 years) were examined. Mean HR during the scanning was 76 ± 16.3 bpm (range, 46–127 bpm). Mean HRV was calculated as 5.6 ± 7.9 bpm. Coronary circulation was right-dominant in 257 patients (90%) and left dominant in 28 patients (10%). Patients referred for coronary CTA ($n=219$, 76%) had a low to intermediate pretest probability for CAD; the remaining 36 (13%) and 30 (11%) patients underwent CTA for coronary stent and coronary bypass-graft(s) patency evaluation, respectively. A total of 56 coronary bypass-grafts were present in 30 patients.

Of 219 patients with referral for coronary angiography with a low to intermediate pretest probability of CAD, 14 patients (6%) had suboptimal stenosis evaluation due to severe calcium burden; among successfully evaluated patients 102 (50%) had no stenosis, 65 (32%) had minimal stenosis (<30%), 17 (8%) had moderate stenosis (30%–49%) and 21 (10%) had significant stenosis ($\geq 50\%$).

When the data of all 285 patients were assessed in 10% increments of the entire R-R interval, all of the coronary segments could be visualized in 277 patients (97%) (Table 1). On a segment-basis, 4265 of the total 4275 coronary artery segments could be assessed, yielding a 99.77% visibili-

Table 1. The number and percentage of patients with visibility or no visibility in all segments of LAD, LCX, and RCA when 10% reconstruction intervals were used throughout the entire R-R interval

Coronary artery	Patients with visibility in all segments	Patients with no visibility in all segments
LAD	284 (99.6)	1 (0.4)
LCX	281 (98.6)	4 (1.4)
RCA	280 (98.2)	5 (1.8)
All coronary arteries	277 (97.2)	8 (2.8)

LAD, left anterior descending artery; LCX, left circumflex artery; RCA, right coronary artery. Data are given as n (%).

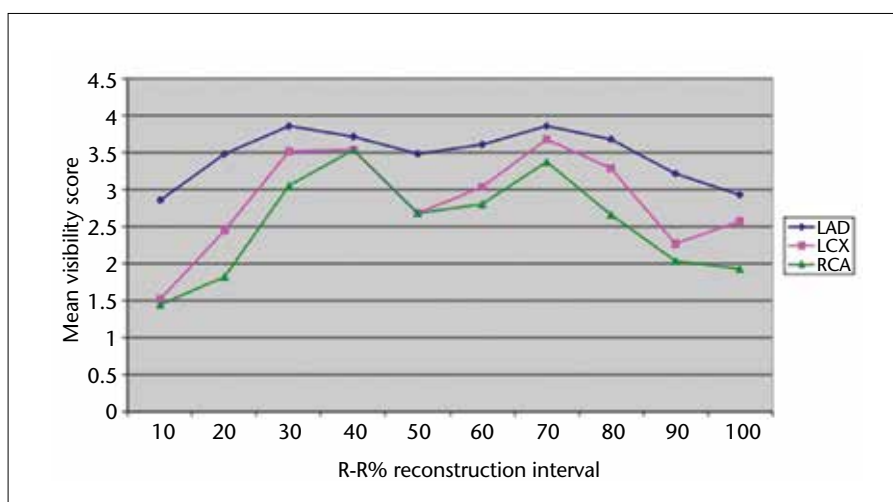


Figure 1. Mean visibility scores of LAD, LCX, and RCA at 10% intervals in all patients. LAD, left anterior descending artery; LCX, left circumflex artery; RCA, right coronary artery.

ty rate. Overall, 10 coronary artery segments in eight patients were not assessable (one segment of LAD, four segments of LCX, and five segments of RCA; one segment each of LAD and LCX not visualized in one patient and one segment each of LCX and RCA not visualized in another patient). Details of these patients were shown in Table 2. Mean HR of these eight patients was higher than the mean HR of the entire study group (88.75 ± 12 bpm vs. 76 ± 16.3 bpm, $P = 0.03$). Whereas, HRV of these eight patients did not show statistical significance compared with the HRV of all patients (8.4 ± 11.4 bpm vs. 5.6 ± 7.9 bpm, $P = 0.33$).

When the data of all 285 patients were evaluated in 10% intervals, maximum mean visibility scores for LAD and LCX were identified at 70% interval; whereas for RCA, 40% was the interval providing the maximum mean visibility score (Fig. 1). The optimal reconstruction interval for evaluation

of all three coronary arteries was 70%, which provided the second highest mean visibility score for evaluation of RCA. In addition, 40% and 30% intervals were also found to be useful for evaluation of all three coronary arteries. The overall visibility of LAD was better than the visibility of LCX and RCA ($P < 0.001$). Total mean segment visibility scores of all coronary arteries were highest at 70%, 40%, and 30% intervals, in decreasing order. There was no statistical significant difference between total mean segment visibility scores obtained at 70% and 40% intervals ($P = 1$). However, the difference between the total visibility scores obtained at 70% and 30% intervals ($P < 0.001$) and at 40% and 30% intervals ($P = 0.037$) were statistically significant.

A similar pattern was observed when the number of patients with full visibility of all the coronary artery segments was examined at 10% datasets (Table 3). If only 70% reconstruction interval

Table 2. Mean heart rate and heart rate variability of the patients with one unevaluable segment of either LAD (n=1), LCX (n=4), or RCA (n=5), when data of all patients were evaluated at 10% increments

Patient no.	LAD		LCX			RCA				
	82	5	82	91	45	48	81	91	116	103
Unevaluable segment no.	6	12	12	11	11	4	2	2	2	2
Mean HR±HRV	102±21.5	105±4.4	102±21.5	83±0.5	101±1.7	83±3.7	84±3	83±0.5	72±1.6	80±31.0

LAD, left anterior descending artery; LCX, left circumflex artery; RCA, right coronary artery; HR, heart rate; HRV, heart rate variability.

Table 3. Distribution of patients in terms of LAD, LCX, and RCA segment-visibility, when 10% reconstruction intervals are used

R-R interval	Coronary arteries	Number of visible segments				
		4	3	2	1	0
10%	LAD	54 (18.9)	152 (53.3)	67 (23.5)	9 (3.2)	3 (1.1)
	LCX	2 (0.7)	34 (11.9)	103 (36.1)	118 (41.4)	28 (9.8)
	RCA	8 (2.8)	21 (7.4)	104 (36.5)	107 (36.5)	45 (15.8)
20%	LAD	164 (57.5)	98 (34.4)	20 (7.0)	2 (0.7)	1 (0.4)
	LCX	34 (11.9)	103 (36.1)	110 (38.6)	32 (11.2)	6 (2.1)
	RCA	11 (3.9)	43 (15.1)	133 (46.7)	80 (28.1)	18 (6.3)
30%	LAD	248 (87.0)	34 (11.9)	2 (0.7)	0 (0.0)	1 (0.4)
	LCX	181 (63.5)	76 (26.7)	25 (8.8)	2 (0.7)	1 (0.4)
	RCA	116 (40.7)	88 (30.9)	67 (23.5)	13 (4.6)	1 (0.4)
40%	LAD	213 (74.7)	63 (22.1)	9 (3.2)	0 (0.0)	0 (0.0)
	LCX	204 (71.6)	49 (17.2)	14 (4.9)	15 (5.3)	3 (1.1)
	RCA	198 (69.5)	56 (19.6)	20 (7.0)	8 (2.8)	3 (1.1)
50%	LAD	164 (57.5)	100 (35.1)	20 (7.0)	1 (0.4)	0 (0.0)
	LCX	97 (34.0)	74 (26.0)	56 (19.6)	41 (14.4)	17 (6.0)
	RCA	77 (27.0)	93 (32.6)	72 (25.3)	34 (11.9)	9 (3.2)
60%	LAD	199 (69.8)	66 (23.2)	17 (5.9)	3 (1.1)	0 (0.0)
	LCX	149 (52.3)	54 (18.9)	38 (13.3)	36 (12.6)	8 (2.8)
	RCA	100 (35.1)	76 (26.7)	73 (25.6)	27 (9.5)	9 (3.2)
70%	LAD	252 (88.4)	28 (9.8)	4 (1.4)	1 (0.4)	0 (0.0)
	LCX	232 (81.4)	26 (9.1)	18 (6.3)	8 (2.8)	1 (0.4)
	RCA	186 (65.3)	48 (16.8)	27 (9.5)	19 (6.7)	5 (1.8)
80%	LAD	213 (74.7)	55 (19.3)	14 (4.9)	3 (1.1)	0 (0.0)
	LCX	171 (60.0)	55 (19.3)	33 (11.6)	19 (6.7)	7 (2.5)
	RCA	98 (34.4)	60 (21.1)	70 (24.6)	46 (16.1)	11 (3.9)
90%	LAD	109 (38.2)	132 (46.3)	38 (13.3)	6 (2.1)	0 (0.0)
	LCX	57 (20.0)	70 (24.6)	72 (25.3)	64 (22.5)	22 (7.7)
	RCA	41 (14.4)	62 (21.8)	84 (29.5)	62 (21.8)	36 (12.6)
100%	LAD	70 (24.6)	137 (48.1)	64 (22.5)	13 (4.6)	1 (0.4)
	LCX	73 (25.6)	95 (33.3)	58 (20.4)	43 (15.1)	16 (5.6)
	RCA	20 (7.0)	59 (20.7)	111 (38.9)	73 (25.6)	22 (7.7)

Data were given as n (%).

LAD, left anterior descending artery; LCX, left circumflex artery; RCA, right coronary artery.

was selected for data acquisition, all segments of LAD, LCX, and RCA could be evaluated in 88.4%, 81.4%, and 65.3% of patients, respectively (Table 3). When using paired combinations of reconstruction intervals, highest

percentage of patients with full visibility could be obtained at 70% and 30% intervals for LAD (97.5% of patients), 70% and 40% intervals for LCX (93.3% of patients), and 70% and 40% intervals for RCA (90.9% of patients) (Table 4).

To assess the relationship between mean HR and segment visibility at different reconstruction intervals, patients were classified into three subgroups: patients with a mean HR <70 bpm (110 patients, 38% of total, mean HR=60.8±6 bpm), patients with a mean HR between 70–100 bpm (149 patients, 52% of total, mean HR=80.8±8 bpm) and patients with a mean HR >100 bpm (26 patients, 9% of total, mean HR=110.3±9 bpm).

When the visibility of the sum of all segments of LAD, LCX, and RCA was assessed in patients with different mean HR categories as described above (Fig. 2), the optimal reconstruction intervals in descending order to visualize the segments of all three coronary arteries were 70%, 60%, 80%, and 30% in patients with a mean HR <70 bpm; 40%, 70%, and 30% in patients with a mean HR between 70–100 bpm; and 40%, 50%, and 30% in patients with a mean HR >100 bpm. In patients with a mean HR <70 bpm, the highest mean visibility score was identified at 70% interval for all three coronary arteries. In patients with a mean HR of 70–100 bpm, the highest mean visibility score was obtained at 30% interval for LAD, and at 40% interval for LCX and RCA. While, in patients with a mean HR >100 bpm, the highest mean visibility scores for LAD, LCX, and RCA were found at 30%, 40%, and 50% intervals, respectively. If only 40% interval was selected for imaging of all three coronary arteries in patients with a mean HR >100 bpm, all segments of LAD, LCX, and RCA could be visualized in 80.8%, 73.1%, and 76.9% of all patients, respectively. Images of selected cases with different HRs are shown in Figs. 3 and 4.

The mean HRs of 25 patients with a LIMA-LAD graft, 13 patients with a saphenous-OM graft, and 10 patients

Table 4. Number and percentage of patients with full visibility in LAD, LCX, or RCA at 70%, 40%, or 30% intervals or any combinations thereof

R-R Interval	LAD	LCX	RCA
70%	252 (88.4)	232 (81.4)	186 (65.3)
40%	213 (74.7)	204 (71.6)	198 (69.5)
30%	248 (87.0)	181 (63.5)	116 (40.7)
70%+40%	275 (96.5)	266 (93.3)	259 (90.9)
70%+30%	278 (97.5)	250 (87.7)	204 (71.6)
30%+40%	267 (93.7)	250 (87.7)	234 (82.1)
70%+30%+40%	282 (98.9)	267 (93.7)	262 (91.9)

Data were given as n (%).

LAD, left anterior descending artery; LCX, left circumflex artery; RCA, right coronary artery.

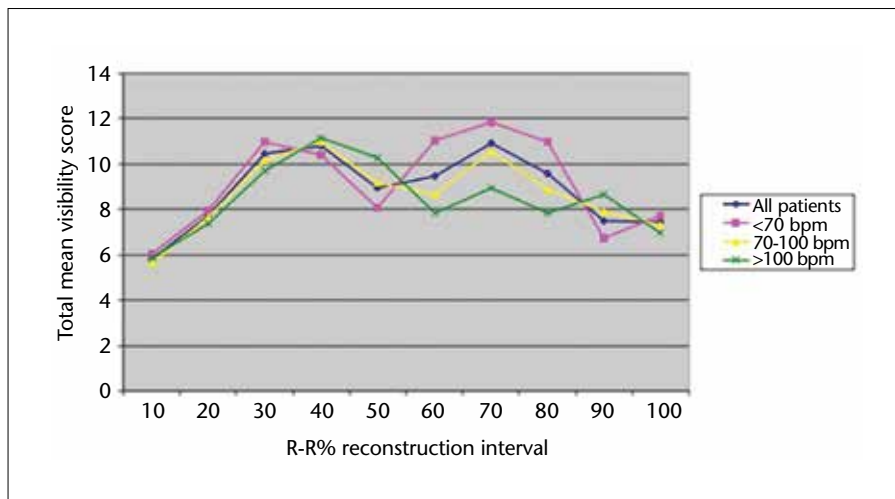


Figure 2. Total mean visibility scores of LAD, LCX, and RCA at 10% intervals, in all patients, in patients with a mean heart rate of <70 bpm, in patients with a mean heart rate of 70–100 bpm, and in patients with a mean heart rate of >100 bpm.

with a saphenous-PDA graft were 76 ± 11 bpm, 76 ± 14 bpm, and 74.2 ± 13 bpm, respectively. In patients with a LIMA-LAD graft, the highest mean graft segment visibility score was 2.92 at 70% interval, followed by 80% interval. The highest mean graft segment visibility scores in 13 patients with 14 saphenous-OM grafts were obtained at 30% interval, while the highest mean graft segment visibility scores in patients with a saphenous-PDA graft were identified at 40% and 70% intervals.

There were no patients with unevaluable bypass-graft segments. The optimal intervals to evaluate LIMA-LAD, saphenous-OM, and saphenous-PDA grafts were 70%, 40%, and 30% intervals, similar to that of the native coronary arteries.

Discussion

Our results drawn from analysis of a relatively large patient group with variable HRs confirmed findings of earlier publications with excellent coronary artery segment visibility (99.77%) determined after assessment of all 10% datasets throughout the entire R-R interval in all 285 patients. Only 10 coronary artery segments in eight patients were not assessable. It was noteworthy that the mean HR of these eight patients (all with a mean HR >70 bpm) was higher than the mean HR of all 285 patients. Thus, patients with mean HR <70 bpm had no unevaluable segments. Previous studies with relatively small patient groups, also demonstrated some decrease in the rate of segment visibility with faster HRs (19, 23). Despite the fact that the patients with unevaluable segments in our study had

a significantly faster mean HR compared to the whole study population, the overall segment visibility could be considered excellent in all subgroups with different mean HRs: 100%, 99.7%, and 98.98% in patients with a mean HR <70 bpm, 70–100 bpm, and >100 bpm, respectively. Most studies assessing coronary artery segments on DSCT coronary angiography, reported 1.3%–2.2% of segments and 2% of patients as unevaluable (15, 16, 19, 24). In these studies coronary segment visibility was assessed in reconstructed datasets from 20% to 80% of the R-R interval in 5% increments (15, 16, 19) and from 35% to 70% of the R-R interval in 5% increments (24) corresponding to the time interval during which full tube current was given.

The mean HRV of the eight patients with unevaluable segments was also slightly higher than all patients, but the difference did not reach statistical significance. Brodoefel et al. (25) reported dependence of image quality on HRV, but not mean HR. In a study including 927 patients, impaired image quality was frequently seen in patients with high HR and severe HRV; however, the image quality between different HR and HRV groups was not statistically significant (26).

The greatest mean visibility score was determined at 70% interval for assessment of LAD and LCX, and at 40% interval for assessment of RCA, if data of all patients were evaluated in single 10% intervals. The optimal reconstruction interval was 70% for assessment of all segments of LAD, LCX, and RCA (which had the second greatest visibility score at 70%). Initial studies with DSCT have also demonstrated that in most of the patients with variable HRs, mid-diastolic intervals provided sufficient image quality (15, 16). In our study, the second and third best visibility scores for assessment of all coronary artery segments were obtained at 40% and 30% intervals, respectively. The combination of 70% and 40% intervals was the best combination providing maximum visibility of all coronary artery segments. It was previously suggested that utilizing both mid-diastolic and end-systolic reconstructions could reduce unevaluable coronary artery segments, particularly at higher HRs (27).

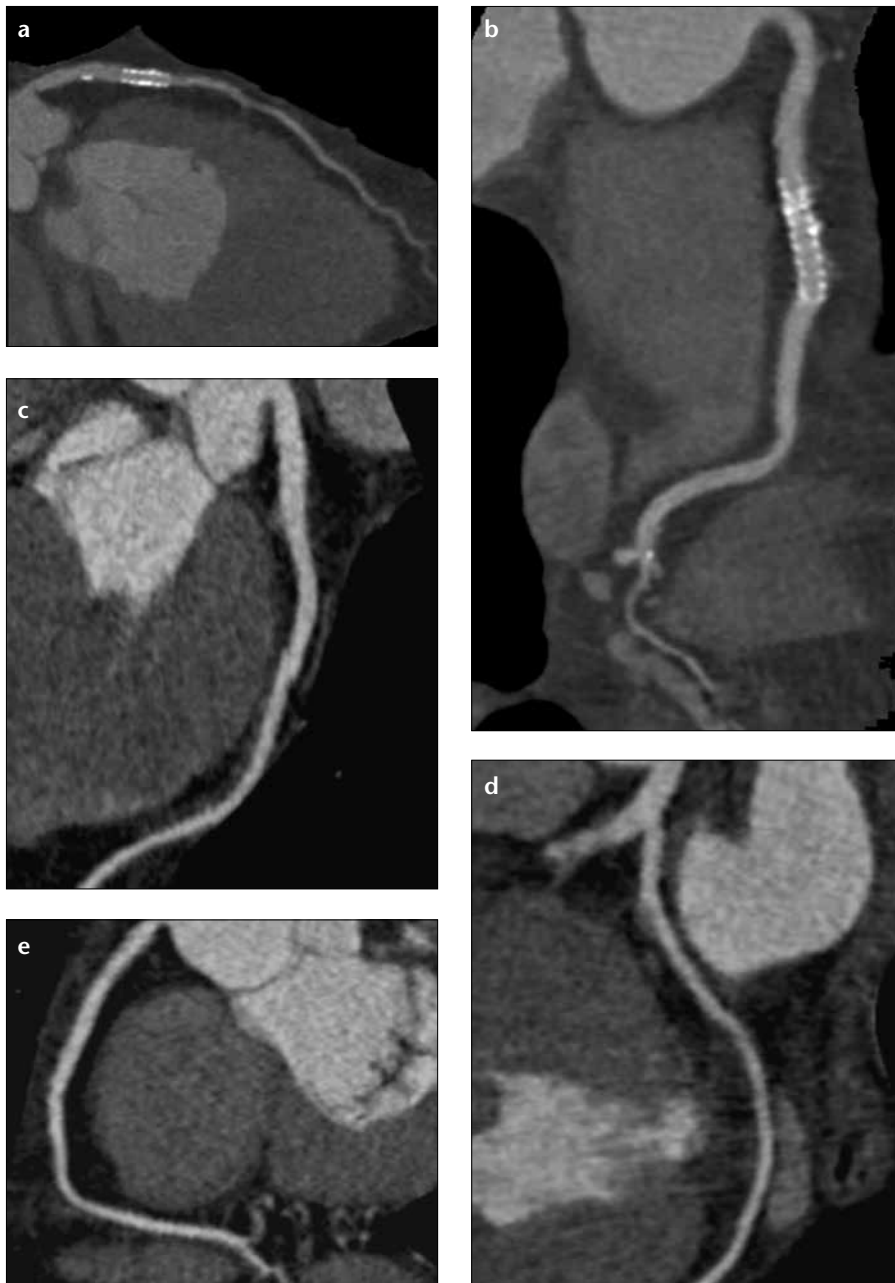


Figure 3. a–e. Multiplanar reconstruction (MPR) images of LAD (a), and RCA (b) of a 57-year-old male patient with a mean heart rate of 64 bpm showing coronary artery segments, along with good visualization of lumen of coronary stents within proximal LAD and RCA. MPR images of LAD (c), LCX (d), and RCA (e) in a 47-year-old male patient with a mean heart rate of 80 bpm depicting corresponding coronary artery segments in high quality.

When we specifically investigated optimal reconstruction intervals for assessment of all coronary artery segments in relation to different HRs, we have come across a similar pattern with prior studies (17), with optimal reconstruction intervals shifting to end-systole with increasing HRs. Relative coronary artery motion during the cardiac phase could be considered the main determinant of coronary

segment visibility on CTA. Husmann et al. (28) evaluated coronary artery motion during cardiac phases in relation to HR using a 64-slice scanner and demonstrated that with increasing HR, mid to late diastolic phase progressively shortens, and at HRs >83 bpm, the smallest coronary velocity shifts from diastole to systole. Other studies using 16-slice and 64-slice scanners assessing influence of HR on image quality sug-

gested that preference of end-systolic reconstructions over mid-diastolic reconstructions would result in better image quality with HRs >65 bpm and >85 bpm, (29, 30). While we did not define a cutoff HR as described in the above studies, our results show that up to 100 bpm, either mid to late diastolic or end-systolic intervals provide acceptable rates of segment visibility. This could be the result of increased temporal resolution. Mid to late diastolic intervals provided better visibility for low HRs (<70 bpm) but were not beneficial for HRs >100 bpm, requiring use of end-systolic intervals in these patients. In a study of 301 patients, 60%–76%, 30%–77%, and 31%–47% intervals were defined as the optimal ECG-pulsing windows for low HRs (≤ 65 bpm), intermediate HRs (66–79 bpm), and high HRs (≥ 80 bpm), respectively, with significant reductions in effective dose for low and high HRs (18). Similar to our results, a recent study by Achenbach et al. (19) predicted that utilizing 70% interval for prospective ECG-gated data acquisition in patients with HR ≤ 60 bpm, would result in acceptable image quality in most cases and this would effectively reduce the radiation exposure. Besides ECG-pulsing and prospectively triggered acquisition, another strategy to reduce radiation exposure would be utilization of a prospectively triggered high-pitch spiral acquisition technique (31). However, low and regular HR is generally considered a prerequisite to obtain superior image quality using this technique. In patients whose HR could not be lowered because of contraindications to beta-blockers, such as overt heart failure, or in patients with insufficient decrease in HR despite beta-blocker use, DSCT with retrospective gating would remain a preferred scan mode; to decrease radiation exposure in these patients, determination of optimal reconstruction intervals for ECG-pulsing is essential. Alternatively, in patients with contraindications or intolerance to beta-blocker use, oral ivabradine premedication could be considered an option to reduce HR prior to coronary CTA (32).

Since bypass-grafts move less rapidly compared to coronary arteries, their visualization with CTA is generally eas-

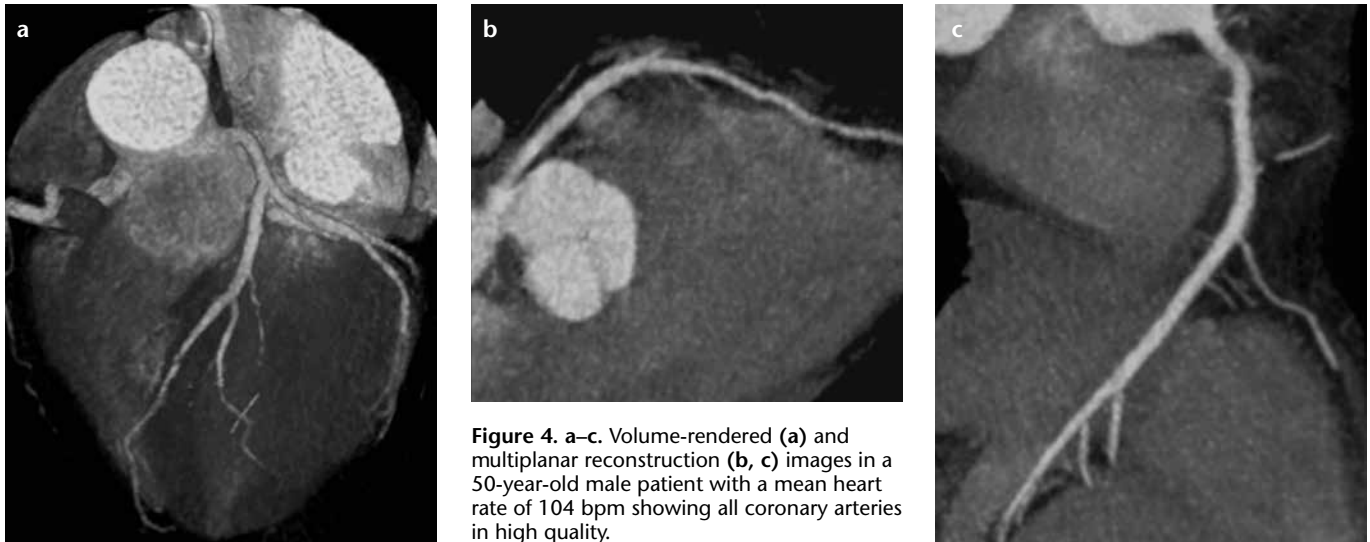


Figure 4. a–c. Volume-rendered (a) and multiplanar reconstruction (b, c) images in a 50-year-old male patient with a mean heart rate of 104 bpm showing all coronary arteries in high quality.

ier to perform than that of native coronary arteries. Visualization rates were reported high, even when using 4-slice scanners (4). On the other hand, arterial grafts may not always be entirely assessable given their small diameter and surgical metallic clip artifacts. In addition, evaluation of distal anastomosis could be challenging because of close proximity to the rapidly moving coronary arteries. In a study by Desbiolles et al. (33) evaluating optimal reconstruction intervals for bypass-graft imaging using 64-slice CT in 25 patients, image quality was significantly better for saphenous venous grafts versus arterial grafts and overall best image quality was found at 60% interval. In our study, all segments of the bypass-grafts were evaluable and there was good segment visibility throughout a wide range of reconstruction intervals. Other DSCT studies, also reported high rates of visibility, with poor image quality in only 2% of arterial grafts and 2% of venous grafts (34). Nevertheless, to our knowledge, no other study in the literature specifically assessed optimal reconstruction intervals for bypass-grafts using DSCT. ECG-controlled tube current modulation gains much more importance during coronary bypass-graft imaging due to wider z-axis coverage. Since bypass-grafts are assessable in a wide range of reconstruction intervals, we recommend determination of ECG-pulsing windows, which would

provide optimal visibility of native coronary arteries.

Our study has a number of limitations. For the image quality evaluation, we took into account only the presence of coronary motion artifacts. Other image-degrading artifacts, such as low signal-to-noise ratio or calcium-related blooming artifacts, were not evaluated. We also did not specifically investigate the effect of coronary calcium burden on overall image quality. Also, since most of our patients were in the low to intermediate likelihood for CAD category, they were not followed up with invasive coronary angiography and thus, we did not have a chance to assess diagnostic accuracy. Lastly, since we utilized ECG-controlled tube current modulation with tube current reduced by 80% during intervals outside 20%–80% R-R reconstruction intervals, segment visibility might have been affected by image noise during intervals with decreased tube current.

In conclusion, our results in a wide population of variable HRs suggest that DSCT coronary angiography, without beta-blocker administration, offers excellent visibility up to 100 bpm HRs using both end-systolic and mid-late diastolic reconstructions and at HRs over 100 bpm using end-systolic reconstructions.

Conflict of interest disclosure

The authors declared no conflicts of interest.

References

1. Hendel RC, Patel MR, Kramer CM, et al. ACCF/ACR/SCCT/SCMR/ASNC/NASCI/SCAI/SIR 2006 appropriateness criteria for cardiac computed tomography and cardiac magnetic resonance imaging: a report of the American College of Cardiology Foundation Quality Strategic Directions Committee Appropriateness Criteria Working Group, American College of Radiology, Society of Cardiovascular Computed Tomography, Society for Cardiovascular Magnetic Resonance, American Society of Nuclear Cardiology, North American Society for Cardiac Imaging, Society for Cardiovascular Angiography and Interventions, and Society of Interventional Radiology. *J Am Coll Cardiol* 2006; 48:1475–1497. [\[CrossRef\]](#)
2. Budoff MJ, Achenbach S, Blumenthal RS, et al. Assessment of coronary artery disease by cardiac computed tomography: a scientific statement from the American Heart Association Committee on Cardiovascular Imaging and Intervention, Council on Cardiovascular Radiology and Intervention, and Committee on Cardiac Imaging, Council on Clinical Cardiology. *Circulation* 2006; 114:1761–1791. [\[CrossRef\]](#)
3. Kantarci M, Doganay S, Karcaaltincaba M, et al. Clinical situations in which coronary CT angiography confers superior diagnostic information compared with coronary angiography. *Diagn Interv Radiol* 2012; 18:261–269.
4. Nieman K, Oudkerk M, Rensing BJ, et al. Coronary angiography with multi-slice computed tomography. *Lancet* 2001; 357:599–603. [\[CrossRef\]](#)
5. Schroeder S, Kopp AF, Kuettner A, et al. Influence of heart rate on vessel visibility in noninvasive coronary angiography using new multislice computed tomography: experience in 94 patients. *Clin Imaging* 2002; 26:106–111. [\[CrossRef\]](#)

6. Giesler T, Baum U, Ropers D, et al. Non-invasive visualization of coronary arteries using contrast-enhanced multidetector CT: influence of heart rate on image quality and stenosis detection. *AJR Am J Roentgenol* 2002; 179:911–916. [\[CrossRef\]](#)
7. Kuettner A, Beck T, Drosch T, et al. Diagnostic accuracy of noninvasive coronary imaging using 16-detector slice spiral computed tomography with 188 ms temporal resolution. *J Am Coll Cardiol* 2005; 45:123–127. [\[CrossRef\]](#)
8. Hoffmann MH, Shi H, Schmitz BL, et al. Noninvasive coronary angiography with multislice computed tomography. *JAMA* 2005; 293:2471–2478. [\[CrossRef\]](#)
9. Wintersperger BJ, Nikolaou K, von Ziegler F, et al. Image quality, motion artifacts, and reconstruction timing of 64-slice coronary computed tomography angiography with 0.33-second rotation speed. *Invest Radiol* 2006; 41:436–442. [\[CrossRef\]](#)
10. Brodoefel H, Reimann A, Burgstahler C, et al. Noninvasive coronary angiography using 64-slice spiral computed tomography in an unselected patient collective: effect of heart rate, heart rate variability and coronary calcifications on image quality and diagnostic accuracy. *Eur J Radiol* 2008; 66:134–141. [\[CrossRef\]](#)
11. Raff GL, Gallagher MJ, O'Neill WW, Goldstein JA. Diagnostic accuracy of noninvasive coronary angiography using 64-slice spiral computed tomography. *J Am Coll Cardiol* 2005; 46:552–557. [\[CrossRef\]](#)
12. Flohr TG, McCollough CH, Bruder H, et al. First performance evaluation of a dual-source CT (DSCT) system. *Eur Radiol* 2006; 16:256–268. [\[CrossRef\]](#)
13. Achenbach S, Ropers D, Kuettner A, et al. Contrast-enhanced coronary artery visualization by dual-source computed tomography--initial experience. *Eur J Radiol* 2006; 57:331–335. [\[CrossRef\]](#)
14. Johnson TR, Nikolaou K, Wintersperger BJ, et al. Dual-source CT cardiac imaging: initial experience. *Eur Radiol* 2006; 16:1409–1415. [\[CrossRef\]](#)
15. Leschka S, Scheffel H, Desbiolles L, et al. Image quality and reconstruction intervals of dual-source CT coronary angiography: recommendations for ECG-pulsing windowing. *Invest Radiol* 2007; 42:543–549. [\[CrossRef\]](#)
16. Matt D, Scheffel H, Leschka S, et al. Dual-source CT coronary angiography: image quality, mean heart rate, and heart rate variability. *AJR Am J Roentgenol* 2007; 189:567–573. [\[CrossRef\]](#)
17. Seifarth H, Wienbeck S, Pusken M, et al. Optimal systolic and diastolic reconstruction windows for coronary CT angiography using dual-source CT. *AJR Am J Roentgenol* 2007; 189:1317–1323. [\[CrossRef\]](#)
18. Weustink AC, Mollet NR, Pugliese F, et al. Optimal electrocardiographic pulsing windows and heart rate: effect on image quality and radiation exposure at dual-source coronary CT angiography. *Radiology* 2008; 248:792–798. [\[CrossRef\]](#)
19. Achenbach S, Manolopoulos M, Schuhback A, et al. Influence of heart rate and phase of the cardiac cycle on the occurrence of motion artifact in dual-source CT angiography of the coronary arteries. *J Cardiovasc Comput Tomogr* 2012; 6:91–98. [\[CrossRef\]](#)
20. Hausleiter J, Meyer T, Hadamitzky M, et al. Radiation dose estimates from cardiac multislice computed tomography in daily practice: impact of different scanning protocols on effective dose estimates. *Circulation* 2006; 113:1305–1310. [\[CrossRef\]](#)
21. Austen WG, Edwards JE, Frye RL, et al. A reporting system on patients evaluated for coronary artery disease. Report of the Ad Hoc Committee for Grading of Coronary Artery Disease, Council on Cardiovascular Surgery, American Heart Association. *Circulation* 1975; 51:5–40. [\[CrossRef\]](#)
22. Gibbons RJ, Chatterjee K, Daley J, et al. ACC/AHA/ACP-ASIM guidelines for the management of patients with chronic stable angina: executive summary and recommendations. A Report of the American College of Cardiology/American Heart Association Task Force on Practice Guidelines (Committee on Management of Patients with Chronic Stable Angina). *Circulation* 1999; 99:2829–2848. [\[CrossRef\]](#)
23. Ropers U, Ropers D, Pflederer T, et al. Influence of heart rate on the diagnostic accuracy of dual-source computed tomography coronary angiography. *J Am Coll Cardiol* 2007; 50:2393–2398. [\[CrossRef\]](#)
24. Rixe J, Rolf A, Conradi G, et al. Image quality on dual-source computed-tomographic coronary angiography. *Eur Radiol* 2008; 18:1857–1862. [\[CrossRef\]](#)
25. Brodoefel H, Burgstahler C, Tsiflikas I, et al. Dual-source CT: effect of heart rate, heart rate variability, and calcification on image quality and diagnostic accuracy. *Radiology* 2008; 247:346–355. [\[CrossRef\]](#)
26. Weustink AC, Neeffes LA, Kyzopoulos S, et al. Impact of heart rate frequency and variability on radiation exposure, image quality, and diagnostic performance in dual-source spiral CT coronary angiography. *Radiology* 2009; 253:672–680. [\[CrossRef\]](#)
27. Sanz J, Rius T, Kuschnir P, et al. The importance of end-systole for optimal reconstruction protocol of coronary angiography with 16-slice multidetector computed tomography. *Invest Radiol* 2005; 40:155–163. [\[CrossRef\]](#)
28. Husmann L, Leschka S, Desbiolles L, et al. Coronary artery motion and cardiac phases: dependency on heart rate -- implications for CT image reconstruction. *Radiology* 2007; 245:567–576. [\[CrossRef\]](#)
29. Herzog C, Arning-Erb M, Zangos S, et al. Multi-detector row CT coronary angiography: influence of reconstruction technique and heart rate on image quality. *Radiology* 2006; 238:75–86. [\[CrossRef\]](#)
30. Leschka S, Wildermuth S, Boehm T, et al. Noninvasive coronary angiography with 64-section CT: effect of average heart rate and heart rate variability on image quality. *Radiology* 2006; 241:378–385. [\[CrossRef\]](#)
31. Lell M, Marwan M, Schepis T, et al. Prospectively ECG-triggered high-pitch spiral acquisition for coronary CT angiography using dual source CT: technique and initial experience. *Eur Radiol* 2009; 19:2576–2583. [\[CrossRef\]](#)
32. Bayraktutan U, Kantarci M, Gundogdu F, et al. Efficacy of ivabradin to reduce heart rate prior to coronary CT angiography: comparison with beta-blocker. *Diagn Interv Radiol* 2012; 18:537–541.
33. Desbiolles L, Leschka S, Plass A, et al. Evaluation of temporal windows for coronary artery bypass graft imaging with 64-slice CT. *Eur Radiol* 2007; 17:2819–2828. [\[CrossRef\]](#)
34. Weustink AC, Nieman K, Pugliese F, et al. Diagnostic accuracy of computed tomography angiography in patients after bypass grafting: comparison with invasive coronary angiography. *JACC Cardiovasc Imaging* 2009; 2:816–824. [\[CrossRef\]](#)